

Defects and acceptor centers in ZnO introduced by C⁺-implantation

M. Jiang · X. D. Xue · Z. Q. Chen ·
Y. D. Liu · H. W. Liang · H. J. Zhang ·
A. Kawasuso

Received: 3 October 2013 / Accepted: 12 November 2013 / Published online: 27 November 2013
© Springer Science+Business Media New York 2013

Abstract ZnO single crystals were implanted with 280 keV C⁺ to a dose of $6 \times 10^{16} \text{ cm}^{-2}$. Positron annihilation measurements reveal a large number of vacancy clusters in the implanted sample. They further agglomerate into larger size or even microvoids after annealing up to 700 °C, and are fully removed at 1200 °C. X-ray diffraction, photoluminescence, and Raman scattering measurements all indicate severe damage introduced by implantation, and the damaged lattice is partially recovered after annealing above 500 °C. From room temperature photoluminescence measurements, an additional peak at around 3.235 eV appears in the implanted sample after annealing at 1100 °C, which is much stronger than that of the free exciton. From the analysis of low temperature photoluminescence spectra, this peak is mostly a free electron to acceptor (e,A⁰) line which is probably associated with C_O.

Introduction

ZnO, as a typical wurtzite semiconductor with direct-band-gap of 3.4 eV, has been found to have prospective

application to optoelectronic devices, such as UV light-emitting diodes and lasers, transparent conducting film, piezoelectric transducers [1, 2]. The large exciton banding energy of 60 meV [3] makes intense near-band-edge (NBE) excitonic emission. However, up to now the stable p-type doping in ZnO is still a difficult task. The possible reason might be due to deep acceptor levels, or the compensation of acceptors by intrinsic defects. Therefore, it is important to investigate the behavior of acceptor levels and their interaction with defects. Photoluminescence has been frequently utilized to explore the donor and acceptor centers which may have been produced by doping. Due to predominance of free exciton (FE) emission at high temperature, recombination of bound excitons associated with donors or acceptors can be observed only from low temperature photoluminescence measurements [4, 5]. However, the chemical origin and binding energy of underlying donor and acceptor species are controversial [6, 7]. Studies from first principles calculations based on density functional theory have not provided convincing explanations due to underestimation of band-gap and uncertainty of the defect energy levels.

Carbon is a common amphoteric impurity in ZnO which is introduced unintentionally during the growth. It is reported to contribute p-type conductivity [8] and is expected to be also related to the green emission [9]. Carbon can be also doped in ZnO by other ways such as ion implantation technique, which is one of the important ways for incorporation of dopants in the selected area at controllable amounts [10, 11]. Impurities such as N have been introduced by implantation which act as shallow acceptors [12]. However, implantation will also introduce large number of defects which may complex the band-edge emissions. Hence, it is important to investigate the recovery process of implantation-induced defects and probable

M. Jiang · X. D. Xue · Z. Q. Chen (✉)
Hubei Nuclear Solid Physics Key Laboratory, Department of
Physics, Wuhan University, Wuhan 430072,
People's Republic of China
e-mail: chenzq@whu.edu.cn

Y. D. Liu · H. W. Liang
School of Physics and Optoelectronic Technology, Dalian
University of Technology, Dalian 116024,
People's Republic of China

H. J. Zhang · A. Kawasuso
Advanced Science Research Center, Japan Atomic Energy
Agency, 1233 Watanuki, Takasaki, Gunma 370-1292, Japan

interaction among these defects. In this paper, we performed positron annihilation and photoluminescence measurements to study the defects and light emission centers in carbon implanted ZnO. We focus on the role of implanted carbon on defect evolution and NBE emission in ZnO.

Experiment

C⁺ ions were implanted into commercially available hydrothermally grown ZnO single crystals (SPC Goodwill) at room temperature, with ion energy of 280 keV and a total dose of $6 \times 10^{16} \text{ cm}^{-2}$. The implanted samples were annealed isochronally in nitrogen from 300 to 1200 °C for 30 min. Positron annihilation, photoluminescence, X-ray diffraction (XRD), and Raman scattering measurements were performed to analyze the microstructure and optical properties of the implanted samples. Details of these measurements can be found in previous papers [13, 14].

Results and discussion

X-ray diffraction

Figure 1 shows the XRD spectra measured for ZnO before and after C⁺ implantation and annealing. The unimplanted ZnO single crystal has good crystallinity of wurtzite structure as indicated by a strong and sharp (002) peak at 34.54°. After C⁺ ion implantation, the (002) peak shifts to

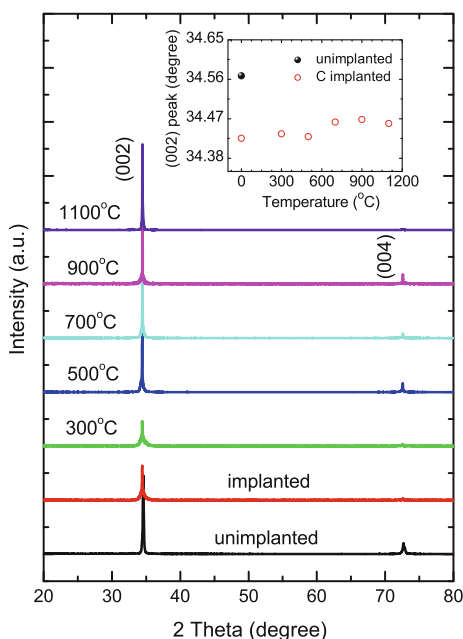


Fig. 1 XRD patterns measured for ZnO before and after C⁺ implantation and annealing. The inset shows the shifts of (002) peak

lower 2θ value, which suggests that C ions possibly substitute O sites and result in increase of lattice parameters. Besides, an obvious decrease of intensity and broadening of the (002) peak can be also observed, which shows that lattice disorder introduced by C⁺ implantation.

After annealing, the (002) peak shows enhancement, but is still broad at annealing temperature below 500 °C. After annealing at 500–700 °C and above the (002) peak has a full recovery. After annealing at 1100 °C, the (002) peak is even narrower than the unimplanted sample, which indicates further improvement of crystal quality. In the whole annealing temperature range, the (002) peak is in lower 2θ value compared to unimplanted ZnO. This reveals that C substitution for O site (C_O) has high thermal stability. No other phase related with the implanted C is observed from the XRD spectra after implantation and annealing at different temperatures.

Positron annihilation measurements

Figure 2a shows the Doppler broadening *S* parameter as a function of incident positron energy (*S*–*E* curves) for the unimplanted ZnO and C⁺ implanted ZnO before and after annealing. The mean implantation depth of incident

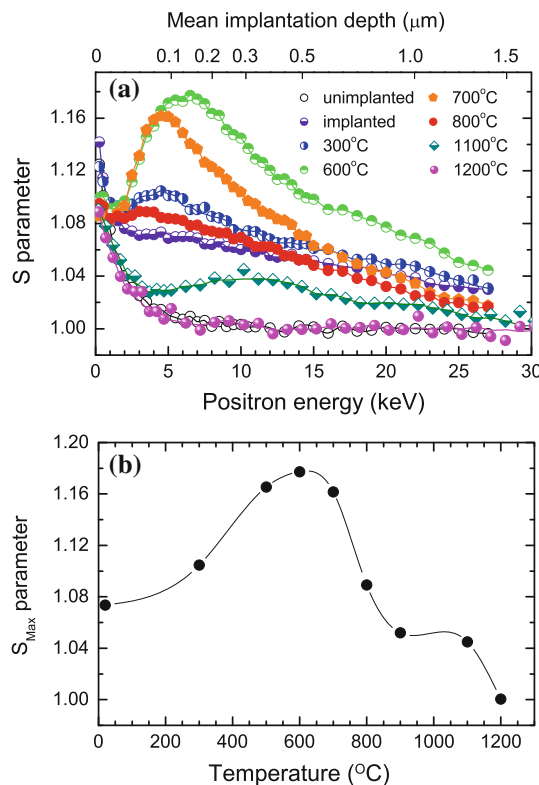


Fig. 2 **a** *S*–*E* curves measured for ZnO before and after C⁺ implantation and annealing. The upper horizontal axis shows the mean implantation depth of positrons for each energy. **b** The maximum *S* parameters in the implanted layer as a function of annealing temperature

positrons is shown on the upper horizontal axis which is calculated by using the following equation:

$$\bar{z} = \frac{AE^n}{\rho}, \quad (1)$$

where E is the positron energy in keV, A and n are constants, and ρ is the material density. In this paper, the values of n and A are 1.6 and $4 \times 10^{-6} \text{ g cm}^{-2} \text{ keV}^{-1.6}$, respectively [15].

For the unimplanted ZnO, the S parameter gradually decreases with increasing energy, and reaches a constant value at $E > 8 \text{ keV}$. This is due to a gradual transfer of positron from the surface state to the deep bulk state with increasing positron energy. After C^+ implantation, the S parameter shows a great increase in the energy range of 3–15 keV, which corresponds to the implanted region of C^+ obtained by Monte Carlo simulation. This suggests large number of vacancy defects introduced by C^+ implantation. After annealing at temperature below 600 °C, the S parameters in the implanted layer show continuous increase, after which they begin to decrease, and finally the S – E curve approaches that of the unimplanted ZnO at 1200 °C.

The maximum S parameters from each S – E curve were selected and plotted as a function of annealing temperature in Fig. 2b. For the as-implanted sample, the S parameter is about 1.07, which indicates that most of the defects are vacancy clusters. At temperatures below 600 °C, the S parameter shows continuous increases, which is a common phenomenon in ion-implanted ZnO and indicates agglomeration of vacancies into larger vacancy clusters. The S parameter attains a rather high value of 1.177 at 600 °C, which means formation of microvoids due to vacancy agglomeration. After increasing annealing temperature to 900 °C, the S parameter abruptly decreases to a value of 1.05, suggesting partial recovery of vacancy clusters or microvoids. At temperature in the range of 900–1100 °C, the S parameter slightly decreases. After annealing at 1200 °C, it approaches the bulk value, which indicates full recovery of vacancy clusters. This recovery temperature is higher than that for other implanted species but nitrogen, which also required similar high temperature to anneal out the damage irrespective of introduction through implantation [16, 17] or different growth ways [18]. The temperature dependence of positron annihilation parameters indicates that such annealing behavior quite likely determined by N [17, 18]. So possibly the vacancy clusters are stabilized by C impurities through formation of complexes in this study.

Raman scattering measurements

Figure 3 shows the Raman spectra measured for ZnO before and after implantation and annealing. For the unimplanted ZnO, there are two phonon modes. The dominant peak at

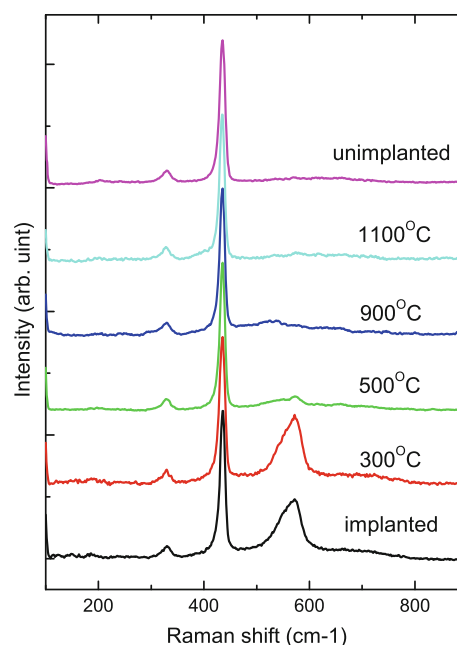


Fig. 3 Raman scattering spectra measured for ZnO before and after C^+ implantation and annealing

437 cm^{-1} is the E_2 (high) mode, which is characteristic of the ZnO wurtzite structure. The peak at 331 cm^{-1} is due to the second-order phonon. After C^+ implantation, A broad peak at around 575 cm^{-1} appears, which is the A_1 (LO) mode and possibly related to defects such as oxygen vacancies [19, 20]. Such broad peak is a typical characteristic in Raman spectra measured for ion-implanted ZnO [10, 11, 13], and indicating high concentration of oxygen vacancies or related defects introduced by implantation. Annealing the implanted sample at 300 °C causes no apparent change of this broad peak. After further annealing at 500 °C, it shows a sharp decrease to much small intensity, This suggests that most of oxygen vacancies are removed at around 500 °C. In general, the 575 cm^{-1} peak was found to be stable up to 700 °C in many ion-implanted ZnO single crystals [13, 10, 21], except for the O^+ implantation, where oxygen vacancies were easily removed at around 400 °C through the recombination of oxygen vacancies and interstitials. Therefore, the moderate thermal stability of oxygen vacancies is clearly due to C ions. The most reasonable explanation is that oxygen vacancies are occupied by C ions at low annealing temperatures, then after annealing at 500 °C, oxygen vacancies are nearly fully recombined with C ions and lead to full recovery of 575 cm^{-1} peak.

Photoluminescence

Figure 4 shows the photoluminescence spectra measured at room temperature for ZnO before and after C^+

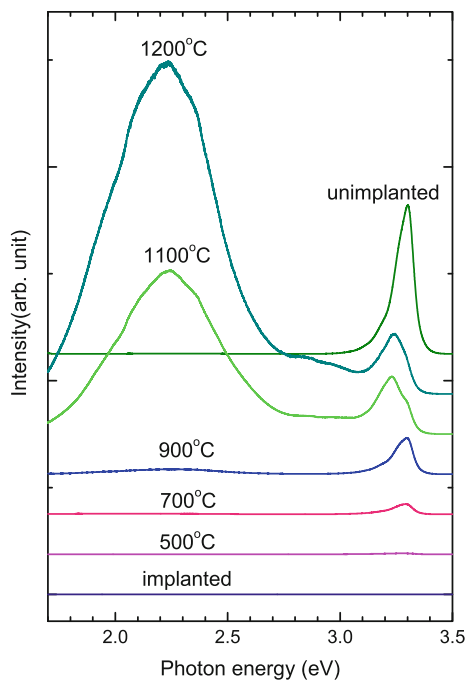


Fig. 4 Room temperature PL spectra measured for ZnO before and after C⁺ implantation and annealing

implantation and annealing. For the unimplanted sample, there is a predominant band-edge UV emission peak and a very weak visible emission, which is attributed to recombination of FE [22, 23] and deep level defects [24], respectively. After C⁺ implantation, both of the two emission bands are completely suppressed. This is apparently due to the implantation-introduced defects, and some of them act as nonradiative recombination centers and compete with the UV and visible emission. Annealing at temperatures below 500 °C has little effect on the PL spectra, indicating that these nonradiative recombination centers are stable at least up to 500 °C. Increasing annealing temperature to 700 °C causes slight recovery of the UV emission peaks, suggesting that some of the non-radiative recombination center are annealed out. After annealing at 1100 °C, the visible emission band shows abrupt increase and becomes very strong at 1200 °C. This means that a high concentration of deep level defects are formed after annealing. The intensity of FE emission also increases above 1100 °C, and strangely, an additional peak at around 3.235 appears and dominates the UV emission.

The coexistence of two peaks in the UV emission band is seldom observed at room temperature in ion-implanted ZnO. Therefore, we performed low temperature PL measurements for this sample to try to find out origin of 3.235 eV emission peak. Figure 5 presents the temperature-dependent PL spectra measured in the NBE region for unimplanted and C⁺-implanted ZnO. Both the two samples are annealed at 1100 °C in nitrogen for comparison. At 10

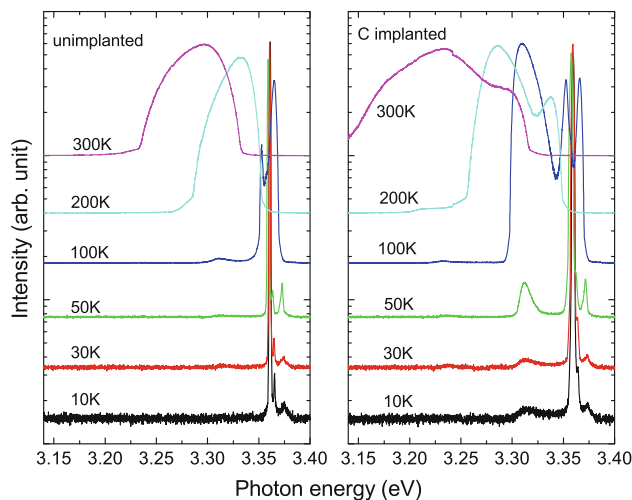


Fig. 5 PL spectra measured at different temperatures for unimplanted and C⁺-implanted ZnO after 1100 °C annealing

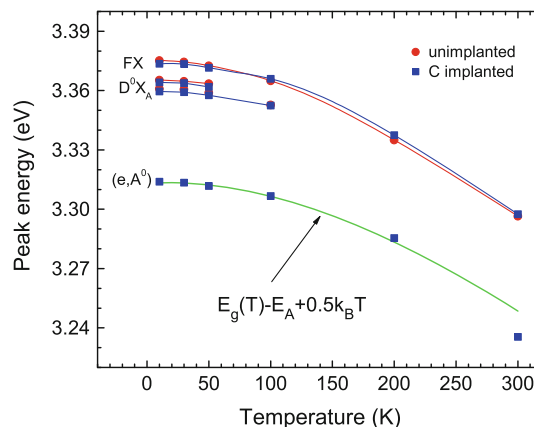


Fig. 6 Positions of all PL peaks as a function of temperature measured for unimplanted and C⁺-implanted ZnO after 1100 °C annealing

K, a FE peak at 3.375 eV and two neutral donor-bound exciton (D^0X_A) at 3.365 and 3.361 eV [25] were observed for unimplanted ZnO. For C⁺-implanted ZnO, besides these three peaks, an additional peak at 3.314 eV appears, and this peak exhibits redshift and increase in width and intensity with increasing temperature. It begins to dominate the whole measured spectrum at 100 K, and two D^0X_A emissions are both quenched above this temperature due to the thermal ionization process. The positions of all these peaks as a function of temperature are plotted in Fig. 6. It can be seen that the peak positions of FE and D^0X_A coincide very well for unimplanted and C⁺-implanted ZnO. Their redshift is due to the decrease of ZnO band-gap with temperature. It is clear that the additional peak is introduced by C⁺ implantation.

The unusual PL peak in C⁺-implanted ZnO is apparently not related to vacancy defects observed by positrons,

since the enhancement of this peak is opposite to the recovery process of vacancy defects. A similar peak has been observed in low temperature PL spectra measured for N doped and undoped ZnO films [26–28]. However the origin of this peak is controversial, as it was assigned to recombination of excitons bound to a neutral acceptor (A^0X) [26] or free electron to acceptor recombination (e, A^0) [27, 28]. The temperature-dependent peak position of this additional emission can be fitted by the following equation [29]:

$$E_{cA}(T) = E_g(T) - E_A + \frac{k_B T}{2}. \quad (2)$$

Here,

$$E_g(T) = E_g(0) - \frac{\alpha T^2}{T + \beta} \quad (3)$$

where α and β are constants. E_A is the acceptor binding energy, and k_B is the Boltzmann constant. It can be seen that the experimental data in Fig. 6 fit well by the above equations. The fitted value of $E_g(0)$, α and β are 3.44 eV, 8.2×10^{-4} eV K^{-1} and 700 K, respectively [29]. The acceptor-binding energy E_A is found to be 127 meV. Based on the above analysis, we believe that the PL peaks at 3.314 and 3.235 eV in our C^+ -implanted ZnO measured at 10 and 300 K, respectively, is related to (e, A^0). The deviation of the fitted line from the data is observed at 300 K, which might be due to the error in determination of the peak position resulting from temperature broadening and the overlap between (e, A^0) and FE emissions.

According to the XRD and Raman measurements, the implanted C^+ ions probably substitute O sites to form C_O . This could be the acceptor involved in the (e, A^0) emission. However, it is strange that the (e, A^0) emission appears only after annealing the C^+ -implanted ZnO at high temperature of 1100–1200 °C. Our positron annihilation results also show that the vacancy defects are removed at around 1100–1200 °C, such high thermal stability of vacancies is most related to C. Therefore a possible explanation is that the C_O is first coupled with implantation-introduced vacancies, so they can survive up to high temperature of 1100–1200 °C. Only after the dissociation of the vacancy–C complexes, the photon emission related with (e, A^0) can be observed. As for the enhancement of visible emission with annealing temperature, its most probable origin is intrinsic defects instead of the implanted carbon, since we observed such phenomenon in many other ion-implanted and even unimplanted ZnO [19, 11, 13, 30].

Hall measurement of the C-implanted ZnO after 1200 °C annealing indicates n-type conductivity. The electron concentration n_e , resistivity ρ , and Hall mobility μ are 1.323×10^{17} cm^{-3} , $0.437 \Omega cm$, and 108 $cm^2 V^{-1} s^{-1}$, respectively. Possible reasons for this discrepancy might be

the donor type impurities or defects, which over compensate these acceptors.

Conclusion

In summary, XRD, positron annihilation, Raman scattering, and PL measurements all indicate lattice damage introduced by C^+ implantation. Most of the defects can be removed after annealing above 500 °C, however, vacancy clusters need a high temperature of about 1200 °C to be annealed out. An additional peak of (e, A^0) found in implanted sample after annealing at 1100 °C. Combining with results of XRD, Raman, slow positron beam, it is mostly related to C_O .

Acknowledgements The authors would like to thank Professors C. X. Pan and G. J. Fang for providing Raman and Hall measurements. This study was supported by the National Natural Science Foundation of China under Grant Nos. 11075120 and 11275143, and the Fundamental Research Funds for the Central Universities under Grant No. 2012202020211.

References

- Vande Pol FCM (1990) Thin-film ZnO-properties and applications. *Ceram Bul.* 69:1959–1965
- Bagnall DM, Chen YF, Zhu Z, Yao T, Koyama S, Sen MY, Goto T (1997) Optically pumped lasing of ZnO at room temperature. *Appl Phys Lett* 70:2230–2232
- Thomas DG (1960) The exciton spectrum of zinc oxide. *J Phys Chem Solids* 15:86–96
- Reynolds DC, Look DC, Jogai B, Litton CW, Collins TC, Harsch W, Cantwell G (1998) Neutral-donor-bound-exciton complexes in ZnO crystals. *Phys Rev B* 57:12151–12155
- Reynolds DC, Look DC, Jogai B, Collins TC (2001) Polariton and free-exciton-like photoluminescence in ZnO. *Appl Phys Lett* 79:3794–3796
- Gutowski J, Presser N, Broser I (1988) Acceptor-exciton complexes in ZnO: a comprehensive analysis of their electronic states by high-resolution magnetooptics and excitation spectroscopy. *Phys Rev B* 38:9746–9758
- Loose P, Rosenzweig M, Wohlecke M (1976) Zeeman effect of bound exciton complexes in ZnO. *Phys Status Solidi b* 75:137–144
- Tan ST, Sun XW, Yu ZG, Wu P, Lo GQ, Kwong DL (2007) P-type conduction in unintentional carbon-doped ZnO thin films. *Appl Phys Lett* 91:072101(1)–072101(3)
- Lu YH, Hong ZX, Feng YP, Russo SP (2010) Roles of carbon in light emission of ZnO. *Appl Phys Lett* 96:091914(1)–091914(3)
- Chen ZQ, Maekawa M, Kawasuso A, Sakai S, Naramoto H (2006) Annealing process of ion-implantation-induced defects in ZnO: chemical effect of the ion species. *J Appl Phys* 99:093507(1)–093507(5)
- Chen ZQ, Kawasuso A, Xu Y, Naramoto H, Yuan XL, Sekiguchi T, Suzuki R, Ohdaira T (2005) Microvoid formation in hydrogen-implanted ZnO probed by a slow positron beam. *Phys Rev B* 71:115213(1)–115213(8)
- Stehr JE, Wang XJ, Filippov S, Pearton SJ, Ivanov IG, Chen WM, Buyanova IA (2013) Defects in N, O and N, Zn implanted ZnO bulk crystals. *J Appl Phys* 113:103509(1)–103509(9)

13. Jiang M, Wang DD, Chen ZQ, Kimura S, Yamashita Y, Mori A, Uedono A (2013) Chemical effect of Si⁺ ions on the implantation-induced defects in ZnO studied by a slow positron beam. *J Appl Phys* 113:043506(1)–043506(7)
14. Liu YD, Liang HW, Xu L, Zhao JZ, Bian JM, Luo YM, Liu Y, Li WC, Wu G, Du GT (2010) Cu related doublets green band emission in ZnO:Cu thin films. *J Appl Phys* 108:113507(1)–113507(4)
15. van Veen A, Schut H, de Vries J, Hakvoort RA, Ijpma MR (1990) Analysis of positron profiling data by means of “VEPFIT”. *AIP Conf Proc* 218:171–196
16. Chen ZQ, Maekawa M, Kawasuso A, Suzuki R, Ohdaira T (2005) Interaction of nitrogen with vacancy defects in N⁺-implanted ZnO studied using a slow positron beam. *Appl Phys Lett* 87:091910(1)–091910(3)
17. Borseth TM, Tuomisto F, Christensen JS, Monakhov EV, Svensson BG, Kuznetsov AY (2008) Vacancy clustering and acceptor activation in nitrogen-implanted ZnO. *Phys Rev B* 77:045204(1)–045204(6)
18. Tuomisto F, Rauch C, Wagner MR, Hoffmann A, Eisermann S, Meyer BK, Kilanski L, Tarun MC, McCluskey MD (2013) Nitrogen and vacancy clusters in ZnO. *J Mater Res* 28:1977–1983
19. Chen ZQ, Wang SJ, Maekawa M, Kawasuso A, Naramoto H, Yuan XL, Sekiguchi T (2007) Thermal evolution of defects in as-grown and electron-irradiated ZnO studied by positron annihilation. *Phys Rev B* 75:245206(1)–245206(9)
20. Exarhos GJ, Sharma SK (1995) Influence of processing variables on the structure and properties of ZnO films. *Thin Solid Films* 270:27–32
21. Chen ZQ, Kawasuso A, Xu Y, Naramoto H, Yuan XL, Sekiguchi T, Suzuki R, Ohdaira T (2005) Production and recovery of defects in phosphorus-implanted ZnO. *J Appl Phys* 97:013528(1)–013528(6)
22. Bagnall DM, Chen YF, Shen MY, Zhu Z, Goto T, Yao T (1998) Room temperature excitonic stimulated emission from zinc oxide epilayers grown by plasma-assisted MBE. *J Cryst Growth* 184/185:605–609
23. Hamby DW, Lucca DA, Klopstein MJ, Cantwell G (2003) Temperature dependent exciton photoluminescence of bulk ZnO. *J Appl Phys* 93:3214–3217
24. Sekiguchi T, Ohashi N, Terada Y (1997) Effect of hydrogenation of ZnO luminescence. *Jpn J Appl Phys* 2(36):L289–L291
25. Teke A, Ozgr U, Dogan S, Gu X, Morkoc H, Nemeth B, Nause J, Everitt HO (2004) Excitonic fine structure and recombination dynamics in single-crystalline ZnO. *Phys Rev B* 70:195207(1)–195207(10)
26. Look DC, Reynolds DC, Litton CW, Jones RL, Eason DB, Cantwell G (2002) Characterization of homoepitaxial p-type ZnO grown by molecular beam epitaxy. *Appl Phys Lett* 81:1830–1832
27. Sun JW, Lu YM, Liu YC, Shen DZ, Zhang ZZ, Yao B, Li BH, Zhang JY, Zhao DX, Fan XW (2007) Nitrogen-related recombination mechanisms in p-type ZnO films grown by plasma-assisted molecular beam epitaxy. *J Appl Phys* 102:043522(1)–043522(6)
28. Chen JJ, Deng XR, Deng H (2013) Progress in the growth and characterization of nonpolar ZnO films. *J Mater Sci* 48:532–542. doi:10.1007/s10853-012-6721-7
29. Wang LJ, Giles NC (2004) Determination of the ionization energy of nitrogen acceptors in zinc oxide using photoluminescence spectroscopy. *Appl Phys Lett* 84:3049–3051
30. Ratheesh Kumar PM, Vijayakumar KP, Sudha Kartha C (2007) On the origin of blue–green luminescence in spray pyrolysed ZnO thin films. *J Mater Sci* 42:2598–2602. doi:10.1007/s10853-006-1339-2